EFDA–JET–PR(12)18

D. Testa, T. Panis, P. Blanchard, A. Fasoli
and JET EFDA contributors

Plasma Isotopic Effect on the Damping Rate of Toroidal Alfvén Eigenmodes with Intermediate Toroidal Mode Numbers

Plasma Isotopic Effect on the Damping Rate of Toroidal Alfvén Eigenmodes with Intermediate Toroidal Mode Numbers

D. Testa[1], T. Panis[1], P. Blanchard[1,2], A. Fasoli[1]
and JET EFDA contributors*

JET-EFDA, Culham Science Centre, OX14 3DB, Abingdon, UK

[1]Ecole Polytechnique Fédérale de Lausanne (EPFL), Centre de Recherches en Physique des Plasmas (CRPP), Association EURATOM – Confédération Suisse, Lausanne, CH
[2]EFDA-CSU, Culham Science Centre, OX14 3DB, Abingdon, OXON, UK
** See annex of F. Romanelli et al, "Overview of JET Results", (23rd IAEA Fusion Energy Conference, Daejon, Republic of Korea (2010)).*

Preprint of Paper to be submitted for publication in
Nuclear Fusion

ABSTRACT.

This paper reports on the results of recent experiments performed on the JET tokamak on Toroidal Alfvén Eigenmodes (TAEs) with toroidal mode number (n) in the range $|n| = 7$. The stability properties of these medium-n TAEs are investigated experimentally using a set of compact in-vessel antennas, providing a direct and real-time measurement of the frequency, damping rate and amplitude for each individual toroidal mode number. The measurements of the damping rate (γ/ω) for these medium-n modes reported here were obtained during a deuterium to helium to hydrogen changeover experimental campaign, and are used to assess to effect of the plasma effective isotopic composition (A_{EFF}) on the stability properties of these medium-n TAEs. We find that the damping rate of $n = 1$ TAEs decreases approximately as $\gamma/\omega \sim 1/A_{EFF}$ as reported previously, but only for modes whose frequency is close to the centre of the $n = 1$ toroidal gap and for density and current profiles giving an open gap structure. Conversely, for $n>5$ TAEs we find that their damping rate approximately increases as $\gamma/\omega \sim A_{EFF}$. The turning point on the γ/ω versus AEFF dependence occurs for $n = 3$ TAEs.

1. INTRODUCTION AND BACKGROUND.

The stability of Alfvén Eigenmodes (AEs) and the effect of these modes on the energy and spatial distribution of fast ions, including fusion generated αs, are among the most important physics issues for the operation of burning plasma experiments such as ITER. Of particular interest are AEs with toroidal mode number (n) in the range $|n| \sim 3$-20, as these are expected to interact most strongly with the αs. The stability of these modes is investigated experimentally in JET using an active system (the so-called Alfvén Eigenmodes Active Diagnostic, AEAD) based on a set of eight compact in-vessel antennas that can be powered with a ± relative phasing, and real-time detection and discrimination of the individual n-components in the measured magnetic spectrum $|\omega\delta B_{MEAS}|(n)$ [1-4]. The AEAD system therefore provides in real-time a direct measurement of the frequency (f_{MEAS}) and damping rate (γ/ω) of the antenna-driven modes during the dynamical evolution of the background plasma parameters, separately for all toroidal mode numbers up to $|n| \leq 5$ [5, 6].

The non-collisional damping of AEs in tokamaks is essentially due to the wave-field energy absorption by the background plasma species (ions and electrons) via Landau damping. This occurs directly, and also through mode conversion of the AE wave-field to kinetic Alfvén waves (KWAs). Various mechanisms have been proposed to explain the overall AE damping [7-15], notably often giving rise to a dependence of the AE mode frequency and damping rate on the effective plasma isotopic composition $A_{EFF} = \Sigma_i n_i A_i / \Sigma_i n_i$, where ni and Ai are the density and mass number of the different plasma ion species, respectively. However, the dependence of f_{MEAS} and γ/ω on A_{EFF} is theoretically predicted to be different when using a fluid or gyro-kinetic model of the global AE wave-field [16]. Fluid models of the plasma [17, 18] predict values of the parallel ($k_{||}$) and perpendicular ($k_{\perp}$) wavenumbers that are independent of the plasma mass, hence the AE angular frequency (ω_{AE}) and the electron Landau damping (γ/ω_{EL}) are given by $\omega_{AE} = k_{||} v_A \propto 1/\sqrt{A_{EFF}}$ and $\gamma/\omega_{EL} \approx k_{\perp}^2 v_s v_A / \Omega_i^2 \exp(-v_A^2/v_{the}^2) \propto \sqrt{A_{EFF}}$ [13] for $v_{thi} < v_A < v_{the}$, where v_A is the Alfvén speed, v_{thi} and v_{the} are the

ion and electron thermal speeds, v_s the sound speed and Ω_i the ion cyclotron angular frequency. Conversely, finite gyro-radius effects introduce a dispersion of the global AE wave-field across the plasma cross-section, so that the AE angular frequency is now given by $\omega_{AE} = k_{||} v_A [1+k_{\perp}^2 \rho_i 2 (3/4+T_e/T_i)]^{1/2}$ [19], where ρ_i is the ion Larmor radius and T_e and T_i are the background electron and ion temperatures, respectively. The small parameter $k_{\perp}\rho i$ introduces an A_{EFF} dependence on ω_{AE} and γ/ω_{EL} that cannot be simply reduced to the $v_A \propto 1/\sqrt{A_{EFF}}$ scaling. Note that for the usual JET experimental conditions where $v_{thi}<v_A<v_{the}$ for all the background thermal ion species, the ion Landau damping on the k^{th}-ion species is approximately given by $\gamma/\omega_{IL,k} \approx \omega\Sigma_l \exp(-1/(2l+1)/\beta_k)/\beta_k$ 3/2 [7, 8], with $l \geq 0$ an integer number. This damping contribution is therefore negligible and only very weakly dependent on A_{EFF} as $\gamma/\omega_{IL,k} \propto (n_e A_{EFF} Z_k / n_k A_k Z_{EFF})^{3/2}$, where Z_k is the atomic charge of the k^{th}-ion species and $Z_{EFF} = \Sigma_i n_i Z^2_i / n_e$ is the plasma effective charge.

Previous measurements of the damping rate for n = 1 TAEs as function of the effective plasma isotopic composition [16] were obtained on the JET tokamak during the clean-up phase following the 1997 Deuterium-Tritium experimental campaign [20]. During this experimental run A_{EFF} was nominally varied in the range $1<A_{EFF}<2.8$, and the damping rate of radially extended n = 1 TAEs was found to decrease for increasing A_{EFF}, in agreement with gyro-kinetic calculations performed with the PENN code [21]. These calculations attributed the global AE damping to the electron Landau damping of the mode-converted kAWs in the low magnetic shear region in the plasma core. Using the new diagnostic capabilities of the AEAD system, and specifically its much improved real-time capabilities, a recent JET experiment [22, 23] where the main ion species was changed-over from deuterium to helium to hydrogen has provided the opportunity to repeat and extend those earlier measurements of the n = 1 TAE damping rate to the more reactor-relevant modes with intermediate toroidal mode number, up to |n| = 15. These new measurements are reported in this work, with the additional aim to motivate further theoretical and modelling analyses similar to those performed in earlier studies conducted within the framework provided by the International Tokamak Physics Activity [3, 24–26].

This paper is then organised as follows. In Section2 we briefly present the experimental scenario and diagnostic techniques used in this work. In Section3 we present the measurements of the damping rate of n = 1, n = 3, n = 4, n = 5 and n = 7 TAEs as function of the effective plasma isotopic composition. Finally, in Section4 we present the conclusions from this experimental study and provide some suggestions that may guide future attempts to interpret theoretically the measurements reported in this work.

2. EXPERIMENTAL SCENARIO AND DIAGNOSTIC TECHNIQUES FOR THE DAMPING RATE MEASUREMENTS DURING THE JET DEUTERIUM TO HELIUM TO HYDROGEN GAS CHANGEOVER EXPERIMENT.

Fuel retention in the plasma walls is one of the main problems that need to be addressed to obtain reliable high-performance operation in tokamaks, particularly when an optimal mixture of deuterium

and tritium is used to produce plasma regimes that aim to achieve a high fusion energy gain. Following the 1997 JET DTE1 experiment [20], a dedicated, 8-months long clean-up campaign was performed to assess tritium retention and removal strategies [27]. As during 2010/2011 the JET first wall was changed from carbon to a metallic one (tungsten with beryllium-coated tiles), a main gas changeover experiment from deuterium to helium to hydrogen was performed to provide a reference point for fuel retention studies previous to operation with a metallic wall. The operational details and the main results of this experiment have been previously reported in [23], and the Readers are referred to this work.

Parasitically to this gas changeover campaign, the AEAD system was used to provide measurements of the frequency and damping rate of TAEs with toroidal mode number in the range $|n| \leq 15$. Data have been analysed for 37 different discharges with an effective plasma mass in the range $1.7 \leq A_{EFF} \leq 3.95$, providing in excess of 10,000 individual damping rate measurements covering a variety of plasma shapes and density, temperature and current profiles. As the gas changeover campaign revolves around a deuterium to helium, and then an helium to hydrogen main ion species changeover, the almost pure He4 discharge Pulse No: 79215 is used as the reference for the damping rate studies reported in this work. Figure1a shows an overview of the main plasma parameters over the active TAE diagnostic time window for this reference discharge: note that this discharge enters into the X-point phase at t = 10.5sec, as indicated by the large increase in the edge magnetic shear. Here $B_{\phi 0}$ is the toroidal magnetic field on the magnetic axis, I_p is the plasma current, q(r) is the safety factor profile (where r is the radial coordinate across the plasma poloidal cross-section and a is the plasma minor radius), s(r) is the magnetic shear profile, $\kappa(r)$ is the elongation profile (with the suffixes "0" and "95" indicating a value on the magnetic axis (r/a = 0) and at 95% (r/a = 0.95) of the normalised poloidal flux), $\delta(r)$ is the average top/bottom triangularity profile, $T_e(r)$ and $T_i(r)$ are the electron and ion temperature profiles (the symbol "<>" indicating a volume-average quantity), $n_e(r)$ is the electron density profile and Z_{EFF} is the plasma effective charge. The top frame of figure 1 shows the value of the antenna-driven radial component of the magnetic field (δB_{ANT}) measured with a pick-up coil (T001) mounted on the low-field side vessel wall, the value of the antenna frequency (f_{ANT}), and the value of the central frequency of the n = 1 TAE gap computed in real-time ($f_{RT} \propto B_{\phi 0\text{-}RT}/R_{GAP}/q_{GAP}/\sqrt{A_{EFF}}/\sqrt{n_{e0\text{-}RT}}$) using the values $R_{GAP} = 3m$ and $q_{GAP} = 1.5$ and a user defined A_{EFF}, without and with ($f_{RT}*I_p = f_{RT}*I_p(t)/\max(I_p)$) normalization with respect to the time evolution of the total plasma current. Figure1b shows the radial profiles for the main background plasma parameters over the active AEAD time window for the reference discharge Pulse No:79215, plotted as function of the square root of the normalised poloidal flux $\psi_N(r) = \psi(r)/\psi(r = a)$. It is immediate to see that a large variety of background plasma conditions are considered in this experimental work.

Regarding the AEAD operational setup, four active antennas were used to drive a B-field perturbation with typical amplitude at the plasma edge $|\delta B_{ANT}| \sim 0.5$mG, i.e. around 10^7 smaller than the toroidal magnetic field used in the experiment. Due to the antenna geometry, a very broad

toroidal spectrum $\delta B_{ANT}(n)$ is excited for any antenna frequency, comprising many components up to $|n| \sim 30$, of which the higher-n ones are more strongly attenuated as the distance from the antennas increases. Figure2 shows the flux-surface averaged value of the antenna-driven radial and poloidal field components for the reference discharge Pulse No: 79215, evaluated at t = 7.50sec (i.e. in the middle of the TAE diagnostic time window) for different toroidal mode numbers. Note that up to two orders of magnitude difference in the antenna-driven magnetic field is seen between its different n-components up to $|n| \leq 30$, which makes it an essential requirement to be able to discriminate in real-time the different components in the measured $|\omega\delta B_{MEAS}|(n)$ spectrum. This is now done both in real-time (on a 1ms time scale) and postpulse [5, 6] using a novel method for mode detection and n-number discrimination that is based on the Sparse Signal Representation theory and the SparSpec algorithm [28, 29].

The measurements of the frequency and damping rate of medium-n AEs have been now routinely obtained in different JET operating scenarios for some time [3, 4, 24-26, 30]. The mode frequency and damping rate can be measured independently for different n-components in a single discharge as the plasma background evolves, thanks to the successful implementation and exploitation of our real-time mode discrimination and tracking algorithm. An example of these measurements is shown in fig3 for the discharge Pulse No:79215, where the AEAD system was configured to drive an odd-n spectrum peaked towards $|n|$=5-11, with a negligible drive for $|n|>15$ and $|n|<3$. Note that measurements for mode numbers above $|n|>15$ cannot be obtained in real-time on a 1ms time scale due to CPU and RAM limitations, and are subject to large error bars due to uncertainties on the magnetic measurements and their full-frequency calibration. The typical uncertainty on the measurement of the mode frequency is within 50Hz, due to the accuracy of the digital synchronous detection system used in the AEAD system. For the accuracy on the determination of the mode numbers one has to consider the possible statistical and systematic errors due to the algorithm used to extract such data. For the data reported in this work, and considering only modes whose (normalized) amplitude is at least 25% of the maximum amplitude in the spectrum, their toroidal mode number can be determined exactly (i.e. $n = n \pm 0$) up to $|n| \sim 10$. The amplitude of such $|n|<10$ modes is then known to within a factor ~2, and the damping rate is subject to an uncertainty of the order of 15% for the typical cases that we consider in our analysis.

3. MEASUREMENTS OF THE DAMPING RATE OF N = 1, N = 3, N = 4, N = 5 AND N = 7 TAES AS FUNCTION OF THE EFFECTIVE PLASMA ISOTOPIC COMPOSITION.

As previously indicated, a large number of different discharges have been considered for the analysis of the dependence of the TAE damping rate on the effective plasma isotopic composition, giving rise to a large scatter in the background plasma profiles. This scatter on one hand clearly complicates the analysis, as the damping rate of medium-n TAEs shows a very subtle dependence on the details of the profiles of the background plasma parameters [30] that may mask the dependencies on A_{EFF}, but on the other hand convincingly allows ascertaining whether any experimental trend is a general

feature of the TAE damping physics and not related to a very peculiar combination of certain values for certain plasma parameters. Figure4 shows an example of the scatter in the electron density and temperature, safety factor, magnetic shear, elongation and triangularity profiles observed in the discharges used for the damping rate analysis reported here. Four discharges are selected (Pulse No: 79215: pure He4; Pulse No: 78978: pure D; Pulse No: 79248: He4 $\rightarrow$ H changeover; Pulse No: 79015: D $\rightarrow$ He4 changeover), and the data are plotted at t = 7.50sec together with the measurement error bar. Apart from the pure D example Pulse No: 78978, the safety profile and the plasma shape are in general well matched between these four reference discharges; conversely, the scatter in the electron density and temperature profiles is typically larger than the error bar on these measurements, with consequences on the value of the measured damping rate [30].

Hence, in order to experimentally assess a possible A_{EFF} dependence of the damping rate for medium-n TAEs, it is important to consider only time points for which at least the continuum [9, 10] and radiative [11] damping mechanisms are expected to be small and furthermore sufficiently similar at all the selected time points. In the limit of a low-β, large aspect ratio plasma ($\varepsilon = a/R_0 << 1$, where R_0 is the position of the magnetic axis, so that $\varepsilon \sim 0.27 \sim \beta$ in JET plasmas), a practical measure of the strength of the continuum damping is given by the radial gradient of the function g(r), where:

$$\left(\gamma/\omega\right)_{CONT} \propto \frac{\Delta_{TAE}}{a}\frac{\delta g(r)}{\partial r},\ g(r) = \frac{1}{\varepsilon_m}\left(\omega^2/\omega_0^2(r) - 1\right) \tag{1a}$$

$$\Delta_{TAE} = \frac{\pi}{8}\frac{r\varepsilon}{m} \propto \frac{1}{8}\frac{ra}{nqR_0},\ \varepsilon_m = \frac{5r_m}{2(R_0 + r_m)}. \tag{1b}$$

Similarly, the radiative damping can be practically estimated as:

$$\left(\gamma/\omega\right)_{RAD} \propto \frac{\varepsilon_m \Delta_{TAE}}{2a}(1 - g^2)\exp\left(-\frac{\Delta(1 - g^2)}{\sqrt{8}\lambda}\right) \tag{2a}$$

$$\lambda = \frac{4m}{r_m^{3/2}}\frac{\partial q}{\partial r}\rho_i\sqrt{\frac{3}{4} + \frac{T_e}{T_i}} \approx \frac{4nq}{r_m\varepsilon^{3/2}}\frac{\partial q}{\partial r}\rho_i\sqrt{\frac{3}{4} + \frac{T_e}{T_i}}. \tag{2b}$$

In the above expressions ω_0 is the central angular frequency of the TAE gap, $\varepsilon = 2\pi f_{ANT}$ is the mode angular frequency, m is the poloidal mode number and r_m is the minor radius position such that $q(r_m) = (2m+1)/2n$. Since the poloidal mode number is not directly measured, m can be replaced with $m \sim nq(r)$ when evaluating numerically eq.(1b) and eq.(2b), and then taking $r_m = r(q = q_{GAP} = 1.5)$.

Figure 5 shows the radial profiles of the g-function and λ-parameter used to evaluate empirically the strength of the continuum and radiative damping mechanisms for an n = 5 mode over the active AEAD time window for the four discharges shown in figure 4. Again, note the significant scatter in these quantities, which may mask any experimental dependence of the TAE damping rate on A_{EFF} if not appropriately taken into account. To this end, we have constructed a reduced database

containing only modes that were measured at time-points with fully relaxed q-profile (sawtoothing plasmas with $q_0<1.0$) and for which $g(r) = \text{mean}(g(r)) \pm \sigma(g)$ and $\lambda(r) = \text{mean}(\lambda(r)) \pm \sigma(\lambda)$, i.e. where the g(r) and $\lambda(r)$ profiles are each within one standard deviation σ of their mean value across the entire database. This effectively is equivalent to consider only cases with a rather open gap structure throughout the entire plasma poloidal cross-section and a relatively low edge magnetic shear $s_{95}<4$, such conditions minimising both the continuum damping at the plasma edge and the overall radiative damping, but without imposing any further specific constraints on the density and temperature profiles. Finally, for statistical purposes we only consider toroidal mode numbers for which there are enough damping rate measurements over any given finite A_{EFF} range, and we empirically quantify this as having at least 20 γ/ω data over any selected $A_{EFF} \pm \text{err}(A_{EFF})/3$ range, where $\text{err}(A_{EFF}) \approx 0.2$ is the typical measurement error on A_{EFF}. This reduced database still includes in excess of 5,000 damping rate measurements, but is now only restricted to modes with $|n| \leq 7$.

The value of the effective plasma isotopic composition A_{EFF} used in this work is taken from the measurement of the TAE mode frequency scaled with respect to the reference almost pure He4 plasma discharge Pulse No: 79215 (see Section-5a in [31] for more details). Further to the analysis presented in [16, 31], here we correct this initial estimate of A_{EFF} to account for the effective charge of the plasma Z_{EFF} [32], specifically to account for the accuracy of the charge-exchange measurements that are used to obtain Z_{EFF} [33]. This correction is important as (even trace) impurities with atomic charge Z_k and mass A_k affect considerably the determination of A_{EFF} when the plasma effective charge is sufficiently different from the nominal one of a pure two main ion species plasmas (with $[n_1, A_1, Z_1]$ and $[n_2, A_2, Z_2]$), i.e. empirically when $Z_{EFF}>1.3*(n_1Z_1^2 + n_2Z_{22})/(n_1Z_1 + n_2Z^2)$. Hence we have that [32].

$$A_{EFF} \approx A_1 \left(\frac{f^{(1)}_{MEAS,N}}{f^{(1,2)}_{MEAS,N}} \right)^2 \left[1 + \frac{Z_*}{n_e A_1} \left(1 - \left(\frac{f^{(1,2)}_{MEAS,N}}{f^{(1)}_{MEAS,N}} \right)^2 \right) \sum_k n_k A_k \right] = A_{EFF,0} \, (1 + \Delta A_{EFF}). \qquad (3)$$

In eq.(3) the index k indicates all the (trace) impurity species with density n_k, $A_{EFF,0}$ is the nominal value of the effective plasma isotopic composition as previously calculated in [16, 31] using the ratio between the measured mode frequency $f_{MEAS,N}$ of an n = N TAE in the reference single main ion (superscript "(1)") and the actual two main ion (superscript "(1,2)") species plasmas, and ΔA_{EFF} is the impurity correction to A_{EFF}, proportional to the non-ideal quantity $Z_* = |Z_e| (Z_1 + Z_2 - Z_{EFF})/Z_1/Z_2$, so that $Z_* = (n_1 + n_2)/n_e$ for a pure two main ion species plasmas, i.e. with $n_k = 0$ for all impurities species.

Figure 6 (a-c) show the experimental measurement of the A_{EFF} dependence of the mode frequency and damping rate for n = 1 TAEs whose frequency is close to the centre of the n = 1 TAE gap, and in the top and bottom part of the gap, respectively. As the frequency width $\Delta\omega/\omega_0$ of the TAE gap is of order $\Delta\omega/\omega_0 \sim \varepsilon$, and in these plasmas the toroidal rotation frequency (f_{TOR}) is usually rather small, with typical values of the order of $f_{TOR} \sim 1$kHz, we empirically consider that a mode is close to the centre of the gap if $|f_{MEAS} - <\omega_0/2\pi + nf_{TOR}>| < \varepsilon/3$ (with <> again indicating a volume-

averaged quantity), whereas it sits in the top (bottom) part of the gap if its frequency is such that $\pm|\, f_{MEAS} - <\omega_0/2\pi + nf_{TOR}>| > \varepsilon/3$, respectively. In figure 6 (and in the following similar figures) the horizontal error bar on A_{EFF} shows $err(A_{EFF})$, i.e. the uncertainty on the experimental measurement of A_{EFF} from the TAE mode frequency, which also includes the error on the charge-exchange measurement of Z_{EFF}; the vertical error bar on the mode frequency (and damping rate) shows the convolution of the measurement error on f_{MEAS} (γ/ω) with the scatter in the all f_{MEAS} (γ/ω) data that were obtained in the $A_{EFF} \pm err(A_{EFF})$ range. Finally, γ/ω data points that appear to be "bunched" together for values of A_{EFF} within $\pm\, err(A_{EFF})/2$ indicate that such measurements were obtained in discharges that had a nominally different isotopic composition but at time points for which A_{EFF} was practically the same. As an example of this bunching of γ/ω measurements, consider the following: the value $A_{EFF} = 2.1$ can be obtained in an almost pure D plasma with an $n_C/(n_C + n_D) = 0.01$ carbon concentration, hence with $Z_{EFF} \sim 1.29$, or in an almost pure H+He4 plasma still with an $n_C/(n_H + n_{He4}) = 0.01$ carbon concentration and with $n_{He4}/(n_H + n_{He4}) \sim 0.33$, giving $Z_{EFF} \sim 1.69$. Finally, note also that the measured mode frequency does not necessarily scale as $f_{MEAS} \propto 1/\sqrt{A_{EFF}}$ as time points with different magnetic field, density and safety factor profiles are considered in this database.

Similarly to the results of [16] for n = 1 TAEs in discharges with low magnetic shear, we find that the damping rate for such modes whose frequency is close to the centre of the toroidal gap decreases for increasing AEFF, as shown in fig6a: this experimental trend is consistent with gyro-kinetic simulations of the global n = 1 TAE wave-field. Conversely, the damping rate of n = 1 TAEs closer to the top continuum increases for increasing AEFF, as shown in figure 6b: this experimental trend is qualitatively consistent with theoretical and numerical calculations using fluid modelling of the global n = 1 TAE wave-field [13, 16-18]. Finally, as shown in figure 6c, γ/ω appears to be largely independent on AEFF for n = 1 TAEs sitting in the bottom part of the gap.

Figures 7 to 10 show the corresponding mode frequency and damping rate measurements for n = 3, n = 4, n = 5 and n = 7 TAEs, using the same format and convention as in figure 6(a-c). Similarly to the case of n = 1 TAEs, for n = 3 TAEs sitting in the bottom part of the gap the damping rate appears to be largely independent on A_{EFF}. Conversely, for n = 3 TAEs whose frequency sits close to the centre or in the upper part of the gap, γ/ω increases for increasing A_{EFF}, with a larger rate $d\gamma(/\omega)/dA_{EFF}$ for the latter class of modes. For n = 4 TAEs the damping rate always increases for increasing A_{EFF}, with a larger rate $d\gamma(/\omega)/dA_{EFF}$ for modes whose frequency sits in the upper part of the gap, similarly to the data obtained for n = 3 TAEs. This general experimental trend of increasing damping rate for increasing A_{EFF} is also obtained for n = 5 TAEs, but with the important difference that $d\gamma(/\omega)/dA_{EFF}$ is now larger for modes whose frequency sits in the bottom part of the gap. Note also that for n = 5 TAEs no measurements are presented for $A_{EFF} < 2$ due to the criteria, mentioned above, that have been employed for assembling the reduced database used for this presentation. Finally, for n = 7 TAEs we again find that the damping rate always increases for increasing A_{EFF}, with a larger rate $d\gamma(/\omega)/dA_{EFF}$ for modes whose frequency sits in the bottom part of the gap, similarly to the measurements obtained for n = 5 modes.

SUMMARY, CONCLUSIONS AND DISCUSSION.

In summary, we have presented here experimental measurements of the dependence of the TAE damping rate on the effective plasma isotopic composition for modes with toroidal mode number up to n = 7. These measurements have been obtained in a variety of plasma configurations with respect to the density, temperature and safety factor profile, which are generally associated to an open gap structure and a low edge magnetic shear, so that the usually largely dominant contributions from the continuum and radiative damping mechanisms could be reduced as far as practically possible.

First, for n = 1 TAEs whose frequency is close to the centre of the gap, we find that $\gamma/\omega \sim 1/A_{EFF}$ as previously observed and calculated using gyro-kinetic modelling of the global n = 1 TAE wave-field in plasmas with low magnetic shear [16]. Second, for higher-n modes whose frequency is close to the centre of the gap, in general we always have that γ/ω increases for increasing AEFF. This experimental trend is qualitatively consistent with calculations from fluid modelling predicting the electron Landau damping (either of the TAE wave-field directly or of the mode converted kAWs) to be the dominant damping mechanism for modes with intermediate mode numbers in low-β plasmas where the usually dominant radiative and continuum damping have been largely avoided. Note however that these earlier results were under-estimating the n = 1 TAE damping rate by a factor ~25 [16]. Third, for modes whose frequency sits closer to the top and/or bottom continuum, we have in general that $\gamma/\omega \sim A_{EFF}$, with the notable exception of the n = 1 TAEs sitting in the bottom part of the gap, for which γ/ω is largely independent on A_{EFF}. Finally, the rate of increase $d\gamma(/\omega)/dA_{EFF}$ is initially larger for modes sitting closer to the top continuum up to n = 4, and then becomes larger for modes sitting closer to the bottom continuum for $n \geq 5$. In these low magnetic shear configurations, the turning point for the γ/ω versus A_{EFF} dependence is found for medium-n modes, with n = 3, which is consistent with previous measurements of the dependence of the damping rate of medium-n TAEs on background plasma parameters [30].

Modelling of the TAE wave-field is beyond the scope of this experimental work, but we feel that our results can be used to provide some suggestions for further theoretical work. Considering the earlier analyses of the medium-n TAE measurements [3, 4, 24-26, 30], we suggest that the different scaling of γ/ω versus A_{EFF} for lower-n modes up to n = 2 and for higher-n modes with n > 3 may be due to the radial localisation and width of their respective Eigenfunction. Low-n modes have typically a global Eigenfunction sampling the entire plasma cross-section, so that in conditions of low magnetic shear mode conversion to kAWs in the plasma core can be the dominant damping mechanism, giving rise to a $\gamma/\omega \sim 1/A_{EFF}$ scaling that has been correctly and quantitatively predicted by the gyro-kinetic code PENN [16]. Conversely, higher-n modes have typically a more localised Eigenfunction that can sit towards mid-radius, hence being less sensitive to most of the mode conversion to kAWs that occurs in the plasma core. For these modes, and in the absence of strong continuum damping, the radiative and the direct electron (and ion) Landau damping mechanisms become more important, hence a general $\gamma/\omega \sim A_{EFF}$ scaling that has been qualitatively (but not quantitatively) predicted using fluid modelling of the TAE wave-field. We cannot test this hypothesis

as the current lack of suitable, high sensitivity internal fluctuations measurements in JET prevents obtaining an experimental measurement of the TAE Eigenfunction. Hence, we propose this tentative explanation for the damping rate measurements reported here for further theoretical analyses.

ACKNOWLEDGEMENTS.

This work was supported by EURATOM under the contract of Association with CRPP-EPFL, and was carried out within the framework of the European Fusion Development Agreement. This work was also partly supported by the Swiss National Science Foundation. The views and opinions expressed herein do not necessarily reflect those of the European Commission. The Authors would like to thank the various members of the CRPP, MIT and JET staff that contributed to the design, installation, commissioning and operation of the AEAD system.

REFERENCES.

[1]. A. Fasoli et al., Physical Review Letters **75** (1995), 645.
[2]. D. Testa, A. Fasoli et al., The new Alfvén Wave Active Excitation System at JET, Proceedings 23rd SOFT Conference (2004); weblink: http://infoscience.epfl.ch/record/143354/files/.
[3]. D. Testa, N. Mellet, T. Panis et al., Nuclear Fusion **50** (2010), 084010.
[4]. T. Panis, D. Testa, A. Fasoli et al., Nuclear Fusion **50** (2010), 084019.
[5]. D. Testa, A. Fasoli, A. Goodyear et al., Fusion Engineering and Design **86** (2011), 381.
[6]. D. Testa, H. Carfantan, A. Goodyear et al., EuroPhysics Letters **92** (2010), 50001.
[7]. R. Betti and J. Freidberg, Physics of Fluids B **4** (1992), 1465.
[7]. L. Villard et al., Nuclear Fusion **32** (1992), 1695.
[9]. F. Zonca and L. Chen, Physical Review Letters **68** (1992), 592
[10]. M.N. Rosenbluth et al., Physical Review Letters **68** (1992), 596.
[11]. R.R. Mett and S.M. Mahajan, Physics of Fluids B **4** (1992), 2885.
[12]. A. Jaun, A. Fasoli and W.W. Heidbrink, Physics of Plasmas **5** (1998), 2952.
[13]. G.Y. Fu et al., Physics of Fluids B **1** (1989), 2404.
[14]. N.N. Gorelenkov et al., Physica Scripta **45** (1992), 163.
[15]. J. Candy et al., Plasma Physics and Controlled Fusion **35** (1993), 957.
[16]. A. Fasoli, A. Jaun and D. Testa, Physics Letters A **265** (2000), 288.
[17]. L. Villard, S. Brunner and J. Vaclavik, Nuclear Fusion **35** (1995), 1173.
[18]. C.Z. Cheng, Physics Reports **1** (1992), 211.
[19]. A. Hasegawa and L.Chen, Physical Review Letters **85** (1975), 370.
[20]. M. Keilhaker et al., Nucear Fusion **39** (1999), 209.
[21]. A. Jaun et al., Computer Physics Communication **92** (1995), 153.
[22]. T. Loarer et al., Journal of Nuclear Materials **415** (2011), S805.
[23]. C. Giroud and K-D. Zastrow, private communication, JET Facilities, 2010.
[24]. D. Testa, N. Mellet, T. Panis et al., Recent JET Experiments on Alfvén Eigenmodes with Intermediate Toroidal Mode Numbers: Measurements and Modelling, Paper EXW/P7-27,

23rd IAEA Fusion Energy Conference, Daejon, Republic of Korea, 11-16 October 2010; weblink: http://infoscience.epfl.ch/record/153045.

[25]. The ITPA Group on Energetic Particles, The Influence of Plasma Shaping on the Damping of Toroidal Alfvén Eigenmodes, Paper THW/P7-08, 23rd IAEA Fusion Energy Conference, Daejeon, Republic of Korea, 11-16 October 2010); weblink: http://infoscience.epfl.ch/record/164163.

[26]. D. Testa, D. Spong, T. Panis, P. Blanchard, A. Fasoli, Nuclear Fusion **51** (2011), 043009.

[27]. N. Bekris et al., Journal of Nuclear Materials **337** (2005), 659.

[28]. S. Bourguignon, H. Carfantan, T. Böhm, Astronomy and Astrophysics **462** (2007), 379.

[29]. A. Klein, H. Carfantan, D. Testa et al., Plasma Physics and Controlled Fusion **50** (2008), 125005.

[30]. T. Panis, A. Fasoli and D. Testa, Analysis of damping rate measurements of Toroidal Alfvén Eigenmodes on JET as a function of n: part-I and part-II, accepted for publication in Nuclear Fusion, January 2012.

[31]. A. Fasoli et al., Physics of Plasmas **7** (2000), 1816.

[32]. D. Testa et al., Determination of the radial profile of the effective plasma isotope mass from measurement of the frequency of Toroidal Alfvén Eigenmodes, in preparation, January 2012.

[33]. C. Giroud et al., Review of Scientific Instruments **79** (2008), 10F525.W

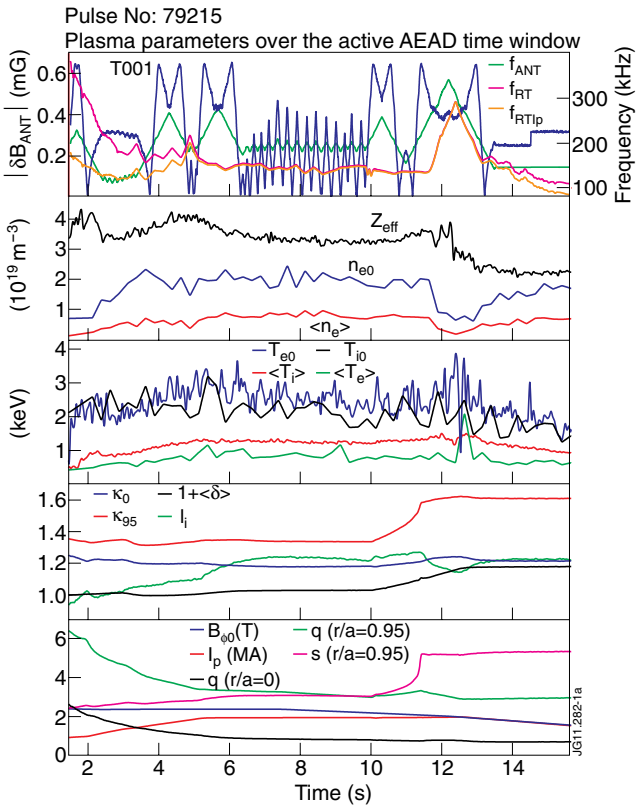

Figure 1: (a) Overview of the main plasma parameters over the active AEAD time window for the reference almost pure He4 Pulse No: 79215.

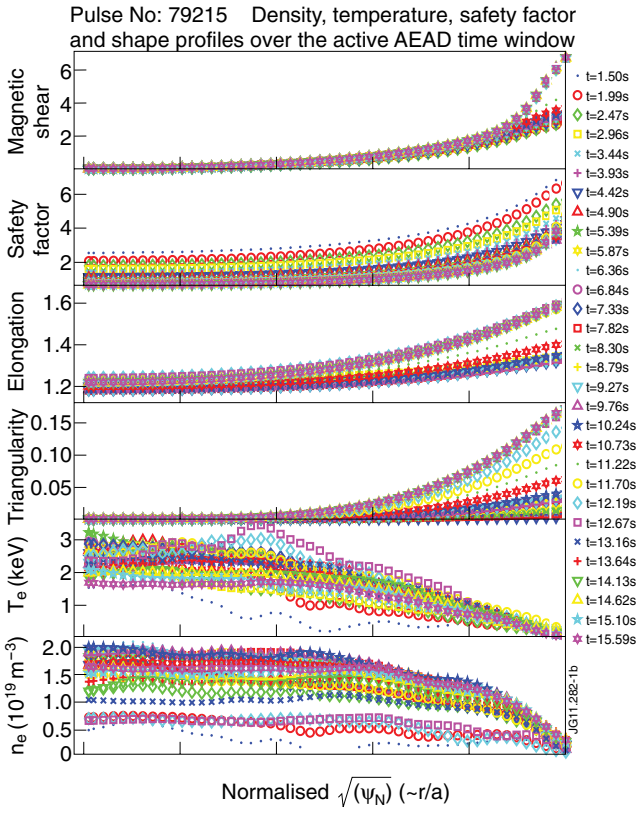

Figure 1: (b) Radial profiles for the main background plasma parameters over the active AEAD time window for the reference almost pure He4 Pulse No: 79215.

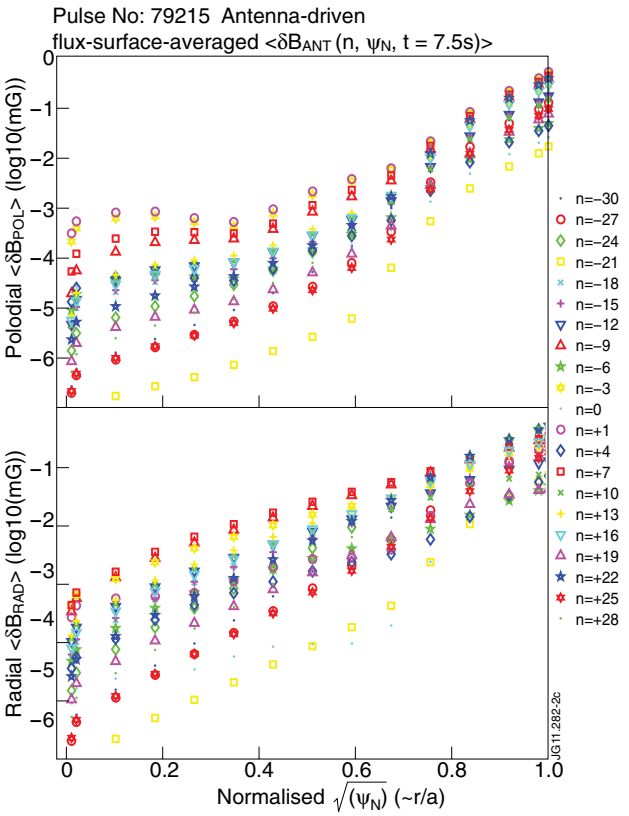

Figure 2: An example of the antenna-driven, flux-surface averaged, radial ($<B_{RAD}(n,\sqrt{\psi_N}(r))>$) and poloidal ($<B_{POL}(n,\sqrt{\psi_N}(r))>$) magnetic field for the Pulse No:79215 at time = 7.50sec for different n-components.

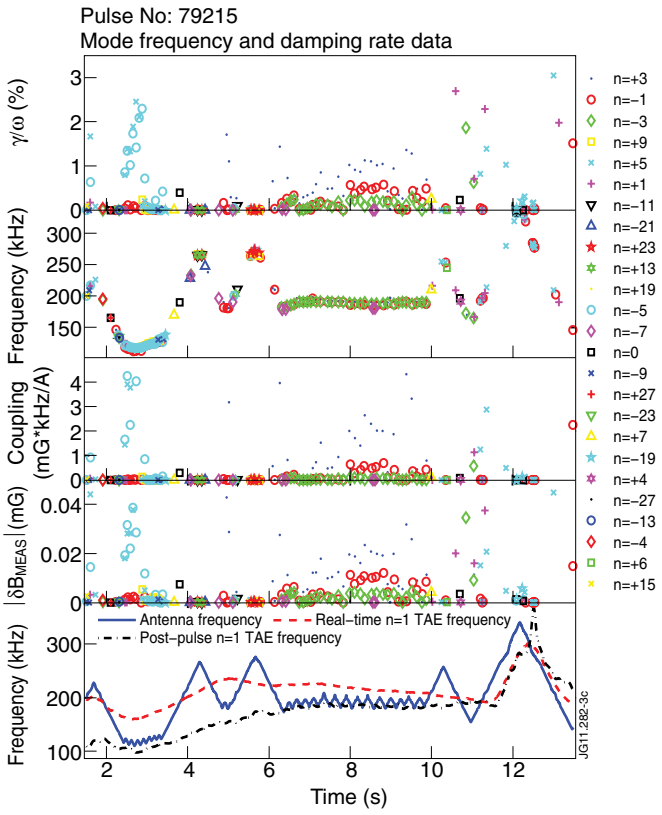

Figure 3: Measurement of the mode frequency and damping rate for TAEs with different toroidal mode numbers for the Pulse No: 79215.

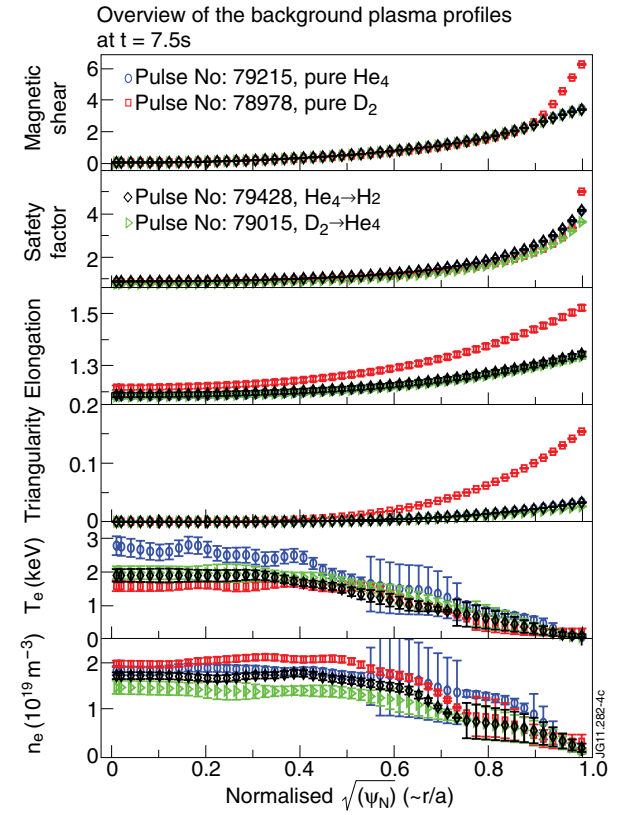

Figure 4: Scatter in the background plasma profiles at t=7.50sec for four illustrative discharges with different A_{EFF} in the gas changeover experiment.

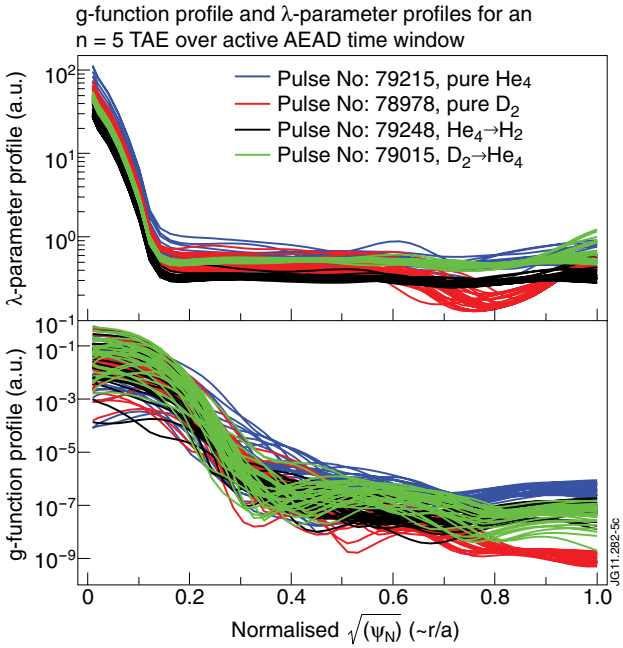

Figure 5: Radial profiles of the g-function and λ-parameter used to evaluate empirically the strength of the continuum and radiative damping mechanisms for an n = 5 TAE.

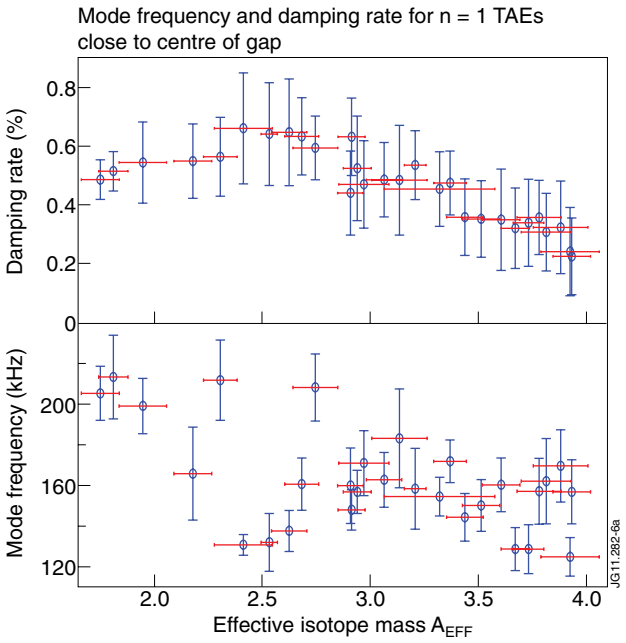

Figure 6: (a) Measurement of the A_{EFF} dependence of the mode frequency and damping rate for n=1 TAEs whose frequency is close to the centre of the n=1 TAE gap, ($|f_{MEAS} - <\omega_0/2\pi + nf_{TOR}>| < \varepsilon/3$.

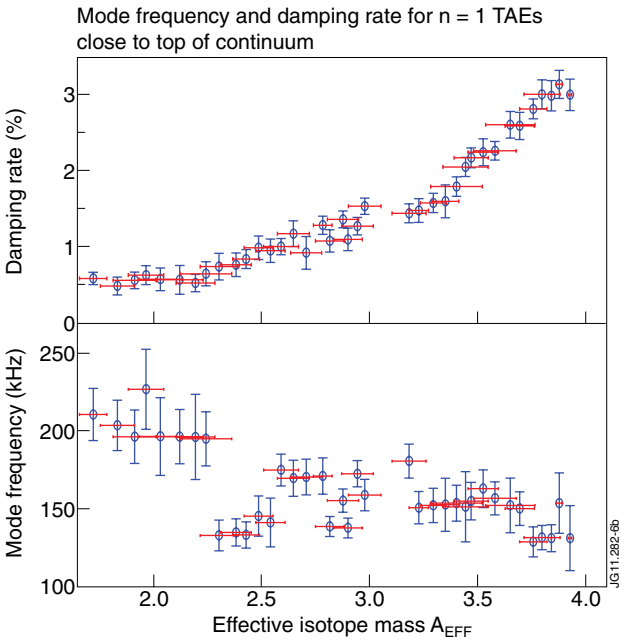

Figure 6: (b) Measurement of the AEFF dependence of the mode frequency and damping rate for n = 1 TAEs whose frequency is in upper part of the n = 1 TAE gap, ($f_{MEAS} - <\omega_0/2\pi + nf_{TOR}> > \varepsilon/3$.

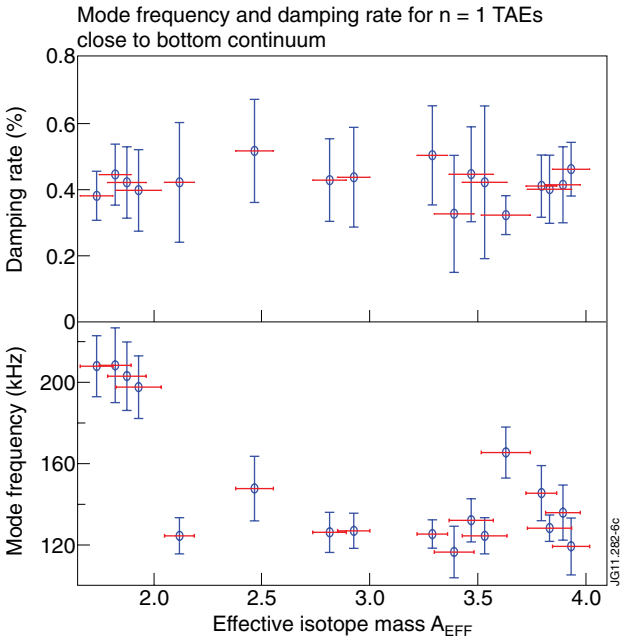

Figure 6: (c) Measurement of the A_{EFF} dependence of the mode frequency and damping rate for n = 1 TAEs whose frequency is in bottom part of the n = 1 TAE gap, ($<\omega_0/2\pi + nf_{TOR}> - f_{MEAS} > \varepsilon/3$.

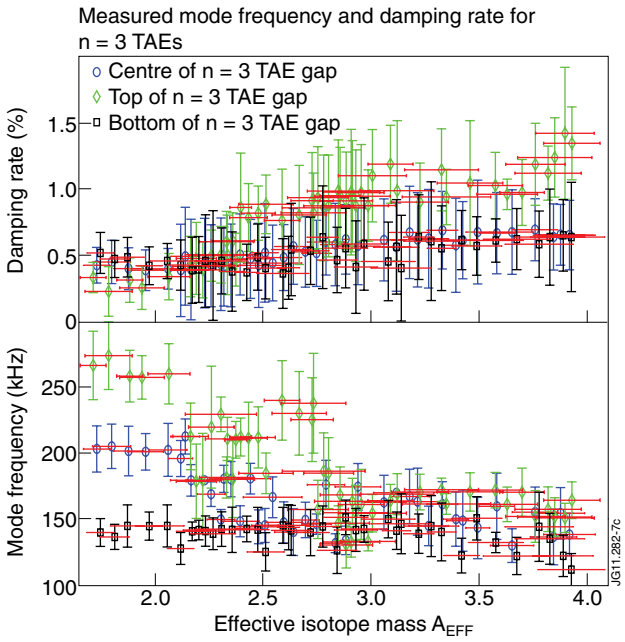

Figure 7: Measurement of the A_{EFF} dependence of the mode frequency and damping rate for n=3 TAEs as function of their position within the gap.

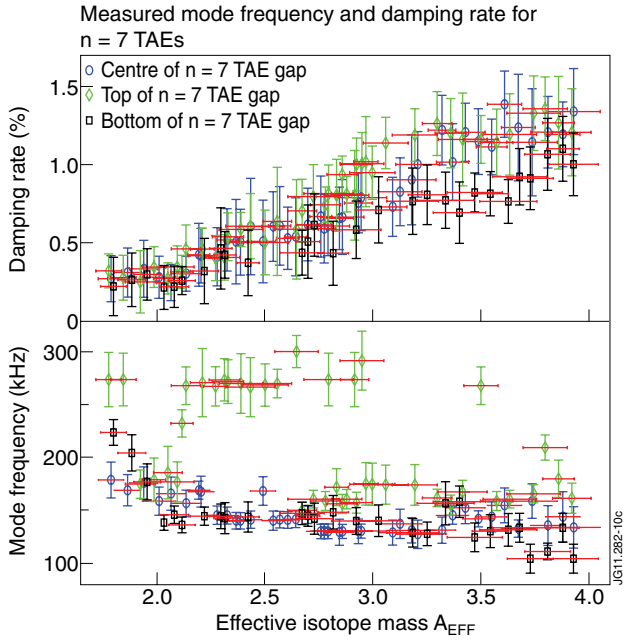

Figure 8: Measurement of the AEFF dependence of the mode frequency and damping rate for n = 4 TAEs as function of their position within the gap.

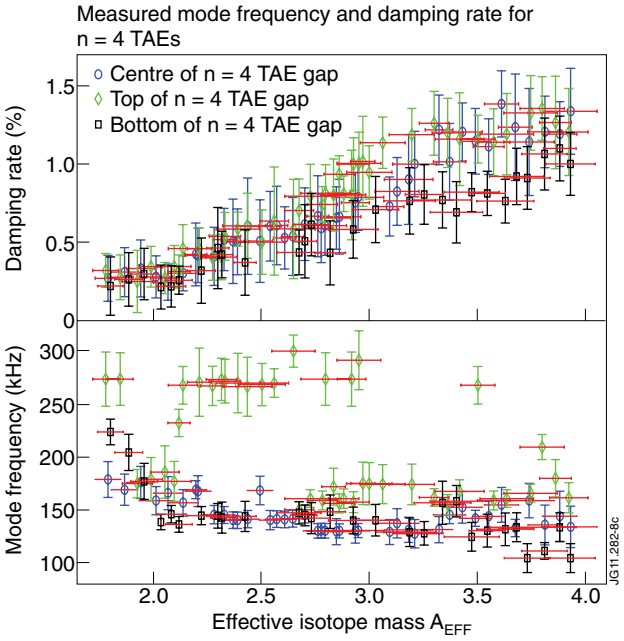

Figure 9: Measurement of the AEFF dependence of the mode frequency and damping rate for n = 5 TAEs as function of their position within the gap.

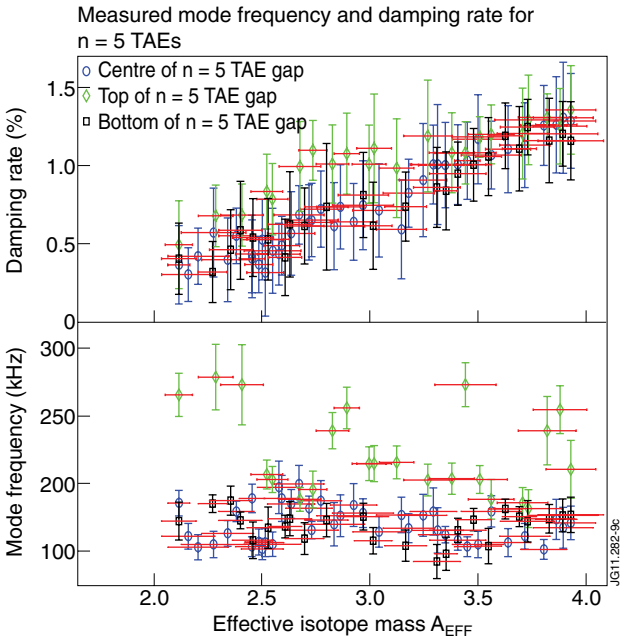

Figure 10: Measurement of the A_{EFF} dependence of the mode frequency and damping rate for n = 7 TAEs as function of their position within the gap.